

SØREN DYBDAL

# Nordic Optical Telescope Scientific Association

## Technical report

OPTICAL SPECIFICATIONS AND PERFORMANCE

of

The Nordic 2.5 m Telescope

Torben B. Andersen

August 1985



OPTICAL SPECIFICATIONS AND PERFORMANCE

of

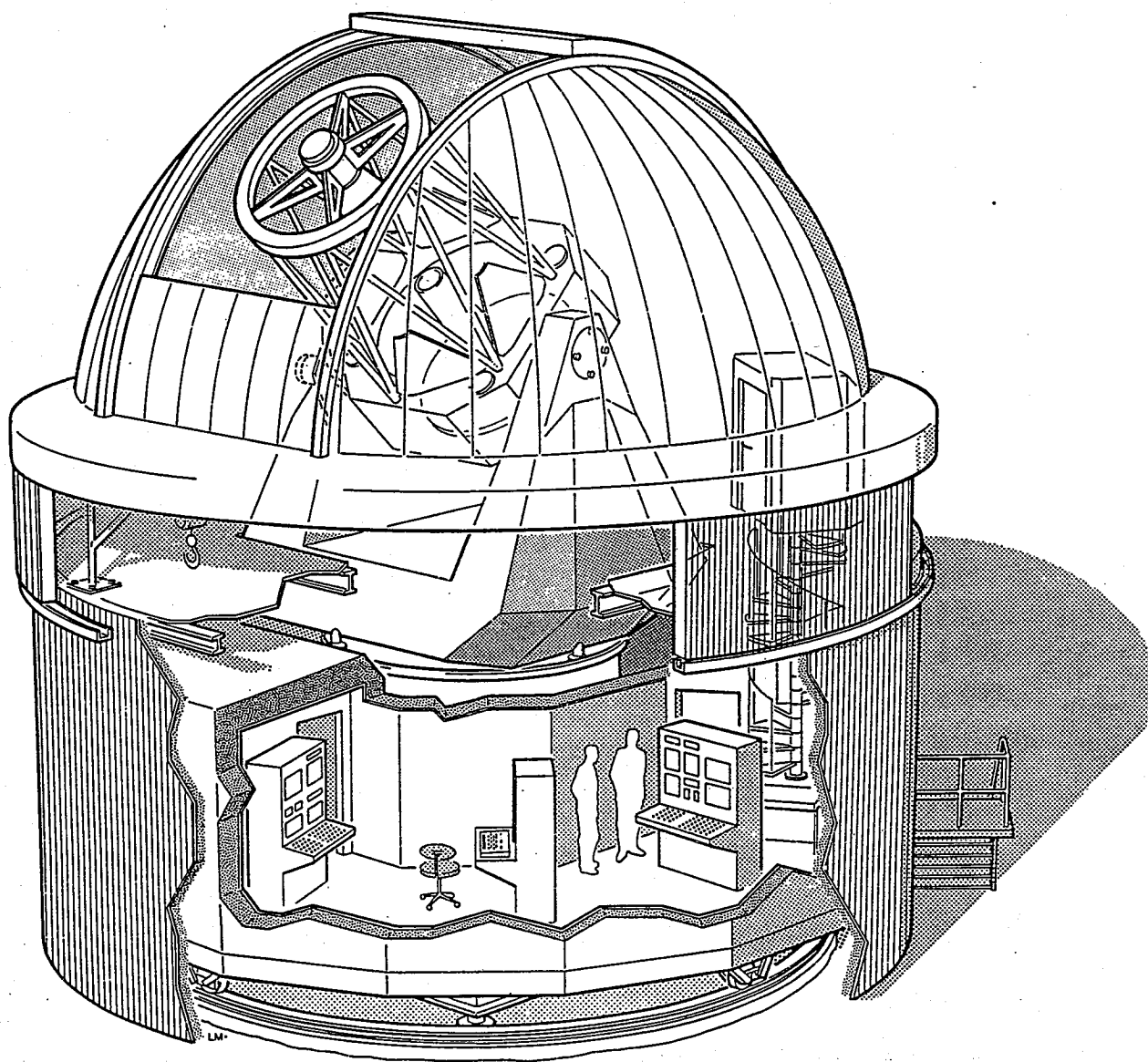
The Nordic 2.5 m Telescope

Torben B. Andersen

August 1985

CONTENTS

	<u>Page</u>
1. INTRODUCTION	2
2. NOTATION USED IN THE GEOMETRICAL DESCRIPTION OF RAYS AND SURFACES	4
3. RITCHEY-CHRÉTIEN TELESCOPES; GENERAL FORMULAS	8
4. SPECIFICATIONS OF THE 2.5 M NORDIC OPTICAL TELESCOPE	11
5. IMAGING PERFORMANCE OF THE 2.5 M TELESCOPE	14
6. TILT-COMPENSATION OF TRANSLATIONAL SHIFT OF SECONDARY MIRROR	17
6.1. Introduction and presentation of notation	17
6.2. Paraxial analysis	18
6.3. Ray trace results	20
6.4. Conclusions	22
7. ASSESSMENT OF THE EFFECTS ON THE GEOMETRIC IMAGE QUALITY DUE TO DEFORMATIONS OF THE TELESCOPE MIRRORS	
7.1. Introduction	33
7.2. Derivation of equations	33
7.3. Applications to 2.5 m telescope deformation calculations	38
8. REFERENCES	41
A. APPENDIX: ABERRATION COEFFICIENTS AND DERIVATIVES FOR THE 2.5 M TELESCOPE	44



The Nordic 2.5 m telescope in its building.

## 1. INTRODUCTION

This report presents the results of geometrical-optical investigations of the 2.5 m Nordic Optical Telescope which is now under construction and will be placed at the Roque de los Muchachos Observatory on the island La Palma, Spain.

The report comprises three previous reports to the NOT-STC Committee (Andersen 1982d, 1984a, 1984b) and resorts extensively to a method and notation developed by the author (Andersen 1980, 1981a, 1981b, 1982a, 1982b, 1982c, 1985) for automatic computation of optical aberration coefficients and their system parameter derivatives.

For a general introduction to modern astronomical optics, telescopes and auxiliary instruments, we refer to papers by Bowen (1967) and Gascoigne (1973). For more systematic treatments on the theory of astronomical telescopes, we refer to Schwarzschild (1905), Chrétien (1922), Wetherell and Rimmer (1972), and Wyman and Korsch (1974a, 1974b, 1975).

Section 2 presents the notation used and outlines the basic formulas for describing the imaging in an optical system. Section 3 gives the general formulas for various important quantities in Ritchey-Chrétien telescopes expressed in terms of basic design parameters. Section 4 gives the specifications for the 2.5 m NOT, whereas Section 5 presents the results of investigations of the imaging performance of the telescope. In Section 6 it is investigated if a translational shift of the secondary mirror can be compensated by a controlled tilt of the secondary, and the result is affirmative. Finally, Section 7 presents a first-order assessment of the effects on the geometric image quality due to deformations of the telescope mirrors.

The design of a correcting element for wide-field photography is not discussed in the present report but will be the subject of a future report. We refer here to papers by Wynne (1965, 1968, 1972) on the design of field correctors for astronomical telescopes. For the 1.54 m Danish Ritchey-Chrétien telescope (f/8.76) located at ESO, La Silla, Chile, a one-element corrector with a symmetric Schmidt corrector profile has been constructed (Andersen and Reiz, 1983). A design of this type is not feasible, however, for the 2.5 m NOT due to a very different value of the difference between the mirror curvatures.

## 2. NOTATION USED IN THE GEOMETRICAL DESCRIPTION OF RAYS AND SURFACES

In this Section we will briefly present the notation used in the description of rays and optical surfaces. For a more detailed description and for the derivation of many of the expressions we refer to Andersen (1980, 1981a, 1981b, 1982a).

We describe the optical system and the propagation of rays in a coordinate system  $(x,y,z)$  where the  $z$ -axis is chosen to correspond with the optical axis for a system with rotational symmetry.

The surfaces are numbered according to the order in which they are met by the light from 1 through  $\Gamma$ .

The surfaces are described by functional expressions:

$$z = z_i + f_i(x,y)$$

where  $f_i(0,0) = 0$ . Hence, for ordinary surfaces with rotational symmetry,  $f_i$  measures the deviation from the polar tangential plane.

We define the axial surface separations

$$d_i = z_{i+1} - z_i$$

The optical materials between the surfaces are considered homogeneous. If, for a refracting surface the refractive indices of the medium before and after refraction at surface  $i$  are  $n_{i-1}$  and  $n_i$ , respectively, we define the relative refractive index as

$$\mu_i = \begin{cases} \frac{n_{i-1}}{n_i} & \text{for a refracting surface} \\ -1 & \text{for a reflecting surface} \end{cases}$$

Rays are specified by the intersection  $(x,y)$  with a plane perpendicular to the  $z$ -axis and by a unit direction vector  $\vec{\sigma} = (L,M,N)$  with  $N > 0$ . Since  $L^2 + M^2 + N^2 = 1$ , it is sufficient to specify the direction tangents

$$\xi = \frac{L}{N}, \quad \eta = \frac{M}{N}.$$

The path of a ray from the initial specification  $(x_0, y_0, \xi_0, \eta_0)$  at a plane  $z = z_0$  in the object space to the final intersection  $(x_{\Gamma+1}, y_{\Gamma+1}, \xi_{\Gamma+1}, \eta_{\Gamma+1})$  with a plane  $z = z_{\Gamma+1}$  in the image space is uniquely determined by the specification  $(f_i, d_i, \mu_i)$  of the optical system.

For a system with rotational symmetry, we can determine functions  $S, T, V, W$  so that

$$\begin{bmatrix} x_{\Gamma+1} & y_{\Gamma+1} \\ \xi_{\Gamma+1} & \eta_{\Gamma+1} \end{bmatrix} = \begin{bmatrix} S & T \\ V & W \end{bmatrix} \begin{bmatrix} x_0 & y_0 \\ \xi_0 & \eta_0 \end{bmatrix}.$$

The aberration functions  $S, T, V, W$  are functions only of the rotation variables

$$\rho_0 = x_0^2 + y_0^2, \quad \psi_0 = \xi_0^2 + \eta_0^2, \quad \kappa_0 = x_0 \xi_0 + y_0 \eta_0.$$

Also, the optical path length of a ray incident on the plane  $z = z_0$  to the image plane  $z = z_{\Gamma+1}$  can be computed

$$\text{O.P.L.} = K(x_0, y_0, \xi_0, \eta_0).$$

For a system with rotational symmetry the optical path length  $K$  is a function only of  $\rho_0, \psi_0, \kappa_0$ :

$$\text{O.P.L.} = K(\rho_0, \psi_0, \kappa_0).$$

The functions S, T, V, W, and K are not in general expressible in closed form. For many purposes, the functions may be expanded in power series which converge reasonably fast. We shall make use of such expansions, for which a general form is

$$\begin{aligned}
 G(\rho_0, \psi_0, \kappa_0) &= \sum_{n=0}^{\infty} \sum_{i=0}^n \sum_{j=0}^i G_{n \ n-i \ i-j \ j} \rho_0^{n-i} \psi_0^{i-j} \eta_0^j \\
 &= G_{0000} + G_{1100} \rho_0 + G_{1010} \psi_0 + G_{1001} \kappa_0 \\
 &+ G_{2200} \rho_0^2 + G_{2110} \rho_0 \psi_0 + G_{2101} \rho_0 \kappa_0 + G_{2020} \psi_0^2 \\
 &+ G_{2011} \psi_0 \kappa_0 + G_{2002} \kappa_0^2 \\
 &+ \dots
 \end{aligned}$$

We refer to Andersen (1980, 1981b) for details on the computation of power series expansion of the functions S, T, V, W, K.

For a point object at infinity in the direction  $(\xi_0, \eta_0)$  it is of interest to consider the center of gravity of the geometric image. The coordinates  $(x_g, y_g)$  in the image plane  $z = z_{\Gamma+1}$  of the center of gravity is defined as

$$(x_g, y_g) = \frac{\iint_{\omega} (x_{\Gamma+1}, y_{\Gamma+1}) dx_0 dy_0}{\iint_{\omega} dx_0 dy_0}$$

where  $\omega$  is the effective entrance pupil in the plane  $z = z_0$ .

Also of great importance is the rms image radius  $k_g$  defined by

$$k_g^2 = \frac{\iint_{\omega} \{(x_g - x_{\Gamma+1})^2 + (y_g - y_{\Gamma+1})^2\} dx_0 dy_0}{\iint_{\omega} dx_0 dy_0}$$

For systems with rotational symmetry and a circular entrance pupil with radius  $R$ , functions  $C_1, C_2$  of  $\sigma = R^2$  and  $\psi_0$  exist so that at the image plane  $z = z_{\Gamma+1} + \Delta$

$$\begin{bmatrix} x_g \\ y_g \end{bmatrix} = (C_1 + C_2\Delta) \begin{bmatrix} \xi_0 \\ \eta_0 \end{bmatrix} .$$

Furthermore, functions  $\pi_0, \pi_1, \pi_2(\sigma, \psi_0)$  may be determined so that at the image plane  $z = z_{\Gamma+1} + \Delta$

$$k_g^2 = \pi_0 + \pi_1\Delta + \pi_2\Delta^2 .$$

The functions  $C_1, C_2, \pi_0, \pi_1, \pi_2$  may be computed from the knowledge of the functions  $S, T, V, W$ .

Finally, the location of the image surface  $z = z_{\Gamma+1} + \Delta_{\min}$  where  $k_g^2$  is a minimum may be determined as

$$\Delta_{\min} = - \frac{\pi_1}{2\pi_2} .$$

We refer to Andersen (1981a) for details on the computation of the functions  $C_1, C_2, \pi_0, \pi_1, \pi_2$ .

### 3. RITCHEY-CHRÉTIEN TELESCOPES; GENERAL FORMULAS

Two-mirror telescopes have been widely used in Astronomy; in particular the Cassegrainian configuration where the distance between the mirrors is shorter than the focal length of the primary mirror.

We refer to papers by Schwarzschild (1905), Wetherell and Rimmer (1972), and Wyman and Korsch (1974a,b,1975) for a general treatment on two-mirror telescopes. Chrétien (1922) found and solved two differential equations for the mirror surface functions  $f_1$  and  $f_2$  satisfying the condition that spherical aberration and coma be zero. This requirement is very important to astronomical applications, providing for symmetric images and reducing magnitude-dependent effects on stellar positions.

The entrance pupil is usually considered coinciding with the primary mirror, thus assuming that all light incident on the primary mirror (except for the secondary shadow) also reaches the image plane. To 3rd-order aberration theory, the two-mirror system is uniquely specified by the distance  $d_1$  from the primary to the secondary, the paraxial surface curvatures  $r_1, r_2$  and the aspherical parameters  $b_1, b_2$ , and the diameter  $D_1$  of the primary mirror aperture. With this notation the surface functions are

$$z - z_i = \frac{1}{2r_i} (x^2 + y^2) + \frac{1+b_i}{8r_i^3} (x^2 + y^2)^2.$$

The zero spherical aberration and zero coma conditions determine the aspherical parameters  $b_1$  and  $b_2$ , leaving  $D_1, d_1, r_1, r_2$  as free parameters. From the designing point of view it is, however, more convenient to specify  $D_1$ , the f-ratio  $F_1$  of the primary mirror, the equivalent f-ratio  $F$  of the entire telescope, and the back-focal distance  $d_b$  which is here to be understood as the distance from the primary mirror plane to the paraxial image plane,  $d_b = z_3 - z_1$ . For practical reasons,  $d_b$  is thought of as being positive.

The dimensions of the secondary are determined by specifying that the telescope should have an unvignetted field of angular radius  $\theta_0$ .

We give a list of important quantities of the telescope expressed in terms of the design parameters  $(D_1, F_1, F, d_b, \theta_0)$ :

telescope equivalent focal length:  $f_{RC} = T_{0000} = D_1 F$

primary mirror paraxial curvature radius:  $r_1 = -2D_1 F_1$

distance from primary to secondary:  $d_1 = \frac{d_b - D_1 F}{1 + \frac{F}{F_1}}$

secondary mirror paraxial curvature radius:  $r_2 = -\frac{2FF_1(d_b + D_1 F_1)}{F^2 - F_1^2}$

primary aspheric parameter:  $b_1 = \frac{D_1(F^3 + 2F_1^3) + d_b(2F_1^2 - F^2)}{F^2(d_b - D_1 F)}$

secondary aspheric parameter:  $b_2 = \frac{(F + F_1)\{D_1 F(F^2 + F_1^2) + d_b(F_1^2 - F^2)\}}{(d_b - D_1 F)(F - F_1)^3}$

diameter of secondary mirror:  $D_2 = \frac{d_b + D_1 F_1}{F + F_1} + 2 \frac{D_1 F - d_b}{1 + \frac{F}{F_1}} \tan \theta_0$

coefficients of 3rd order field-curvature and astigmatism:

$$S_{1010} = \frac{(2F^2 - F_1^2)(d_b - D_1 F)}{4FF_1(d_b + D_1 F_1)}$$

$$T_{1001} = -\frac{D_1 F(2F + F_1) + d_b F_1}{2F(d_b + D_1 F_1)}$$

sagittal focal curvature:  $\frac{1}{r_s} = \frac{2}{f_{RC}} S_{1010}$

tangential focal curvature:  $\frac{1}{r_t} = \frac{2}{f_{RC}} (S_{1010} + T_{1001})$

compromised focal curvature:  $\frac{1}{r_f} = \frac{1}{2} \left( \frac{1}{r_s} + \frac{1}{r_t} \right) = \frac{1}{f_{RC}} (2S_{1010} + T_{1001})$

Due to the curvature of the field only a very limited plane field of good definition is achieved in the Gaussian focal plane. To obtain a plane field of angular diameter  $2\theta$  the focal plane must be shifted the amount  $\Delta d_b$  until the image aberration at the field centre equals that at the edge. Wynne (1968) has given very useful formulas for the shift  $\Delta d_b$  and the maximum image spread  $\delta u$  (in radians) over the field:

$$\Delta d_b = \frac{f_{RC}^2}{4r_t} \tan^2 \theta = \frac{1}{2} f_{RC} (S_{1010} + T_{1001}) \tan^2 \theta.$$

$$\delta u = -\frac{D_1}{f_{RC}} \frac{\Delta d_b}{2} = -\frac{1}{2F} (S_{1010} + T_{1001}) \tan^2 \theta.$$

Usually, the focus position on astronomical two-mirror telescopes is controlled by shifting the secondary mirror rather than shifting the focal plane itself. A shift  $\Delta d_b$  of the focal plane corresponds to a shift  $\Delta d_1$  of the secondary determined by

$$\Delta d_1 = -\frac{\Delta d_b}{1 + \left(\frac{F}{F_1}\right)^2}.$$

#### 4. SPECIFICATIONS OF THE 2.5 M NORDIC OPTICAL TELESCOPE

The 2.5 m Nordic Optical Telescope is specified as a strict Ritchey-Chrétien system with design parameters

$$(D_1, F_1, F, d_b, \theta_0) = (2560 \text{ mm}; 2.0; 11.0; 962 \text{ mm}; 12!5).$$

From these basic parameters we can derive the quantities discussed in Section 3. We get

$$\begin{aligned} \text{Focal length of telescope: } f_{RC} = T_{0000} &= 28160 \text{ mm/rad} \\ &= 136.52 \text{ } \mu\text{m/}^\circ \end{aligned}$$

$$\text{Reciprocal plate scale: } f_{RC}^{-1} = 7.325 \text{ }^\circ/\text{mm}$$

$$\text{Distance from primary to secondary: } d_1 = -4184.308 \text{ mm}$$

Paraxial radii of curvature of mirrors:

$$r_1 = -10240 \text{ mm}; r_2 = -2287.248 \text{ mm}$$

Aspheric parameters of mirrors:

$$b_1 = -1.014785; b_2 = -2.234127$$

$$\begin{aligned} \text{Secondary mirror diameter } D_2 &= 498.28 \text{ mm} \\ (\text{on-axis illuminated diameter} &= 467.85 \text{ mm}). \end{aligned}$$

Coefficients of field-curvature and astigmatism:

$$S_{1010} = -12.0944; T_{1001} = -5.0653$$

Field curvatures:

$$r_s = -1164.2 \text{ mm}; r_t = -820.5 \text{ mm}; r_f = -962.6 \text{ mm}.$$

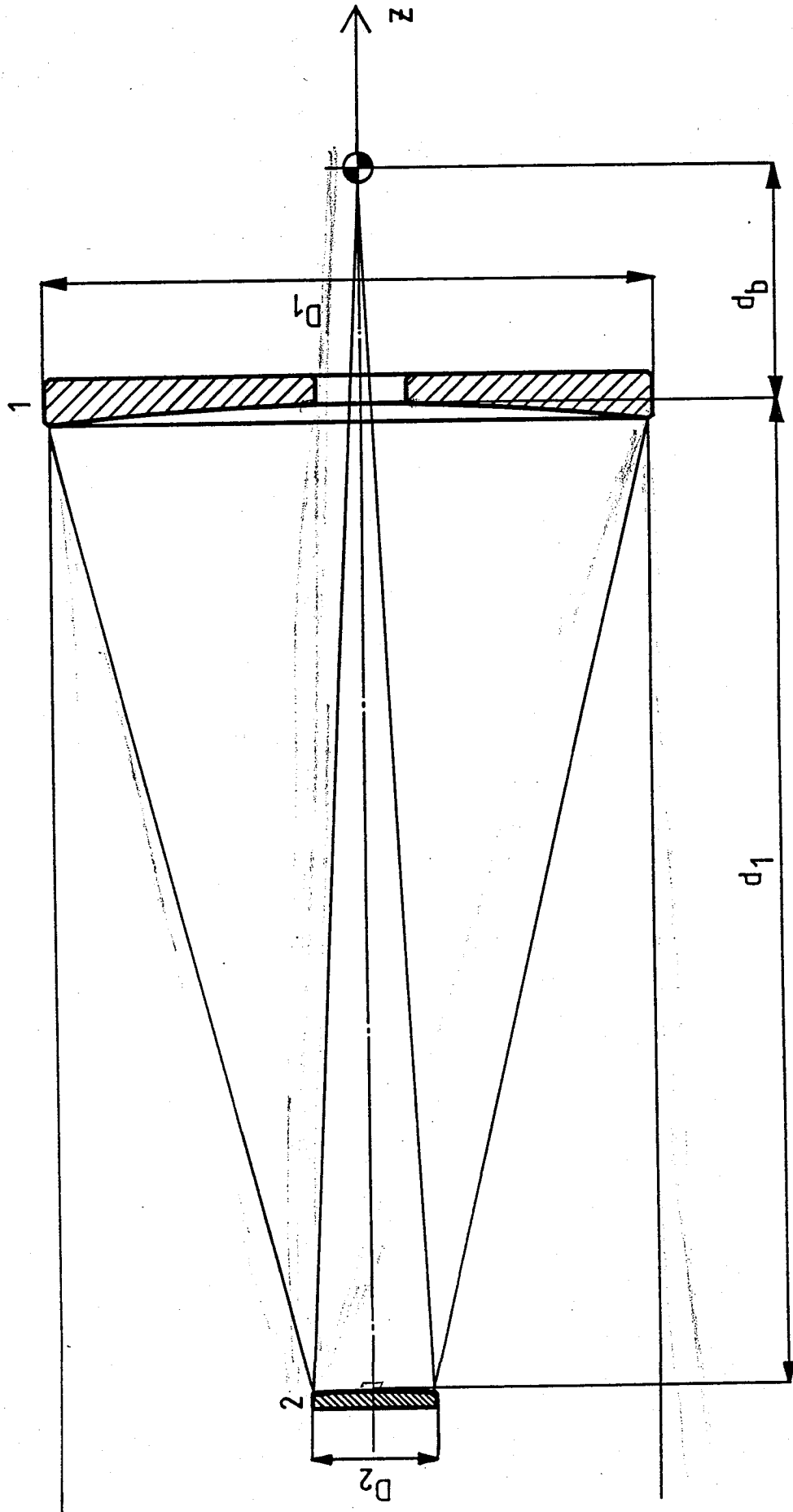


Fig. 4-1. The mirror configuration of the 2.5 m telescope.

Coefficient of distortion:

$$T_{1010} = 150735.9 \text{ mm}$$

The polynomial expressions for the mirror surface functions are (expressed in mm-units):

$$\text{Primary: } f_1 = - 4.8828125 \times 10^{-5} r^2 + 1.721171778 \times 10^{-15} r^4 - 1.213412266 \times 10^{-25} r^6$$

$$\text{Secondary: } f_2 = - 2.186033303 \times 10^{-4} r^2 + 1.289229214 \times 10^{-11} r^4 - 1.520664817 \times 10^{-18} r^6$$

where  $r$  is the radial distance from the optic axis in the mirror vertex tangential plane. We note that the 3rd term of the primary surface equation contributes only  $5 \times 10^{-7}$  mm to the surface deviation at the  $r = 1280$  mm edge and is hence generally negligible. The 3rd term of the secondary surface equation contributes  $3.6 \times 10^{-4}$  mm at the edge of the  $r = 249.1$  mm zone.

Appendix A presents the aberration coefficients for the telescope, i.e., the expansion coefficients for the functions  $S, T, V, W$  to the 5th order. Also given are the derivatives of the aberration coefficients with respect to the design parameters  $r_1^{-1}, r_2^{-1}, b_1, b_2$ .

5. IMAGING PERFORMANCE OF THE 2.5 M TELESCOPE

We have studied the geometric-optical imaging properties of the 2.5 m Nordic Optical Telescope. To present a general overview of the effects of field-curvature and astigmatism, we give in Table I the amounts  $\Delta d_b$  (or  $\Delta d_1$ ) which the image plane (or the secondary mirror) must be shifted in order to achieve an optimized field of angular radius  $\theta$ . Also given are the maximum image blur  $\delta u$ , the radius  $y_\theta$  of the field, and the vignetting  $v_\theta$  at the edge of the field (i.e., the relative amount of light from the primary which misses the secondary).

Table 1.

$\theta$	$2\theta$	$\Delta d_b$	$\Delta d_1$	$\delta u$	$y_\theta$	$v_\theta$
0'	0'	0.0000mm	0.0000mm	0"000	0.0 $\mu$ m	0.000mm 0 %
2.5	5	-0.1278	+0.0041	0.085	11.6	20.479 0
5.0	10	-0.5111	0.0164	0.340	46.5	40.957 0
7.5	15	-1.1500	0.0368	0.766	104.5	61.436 0
10.0	20	-2.0444	0.0654	1.361	185.9	81.914 0
12.5	25	-3.1944	0.1022	2.127	290.4	102.393 0
15.0	30	-4.6000	0.1472	3.063	418.2	122.872 0.30%
17.5	35	-6.2611	0.2004	4.169	569.2	143.351 0.80%
20.0	40	-8.1778	0.2617	5.445	743.4	163.830 1.38%

In order to study the imaging properties in more detail, we used the calculated aberration functions to compute rms image radii  $k_g$  for different positions of the secondary mirror corresponding to various optimized field sizes also covered by Table 1. The results are presented in Table 2 which also gives quantities related to the focal surface minimizing  $k_g^2$ , and the functions  $C_1, C_2, \pi_0, \pi_1, \pi_2$ .

We notice, that at the moderate aperture ratio ( $f/11$ ) and field sizes ( $\theta \approx 0.25$ ) 3rd order aberration theory provide a very adequate description of the imaging properties. Including also 5th order aberration coefficients gives a complete description. Aberration coefficients of 7th and higher orders are completely negligible.

Table 2.

PROPOSED 2.56-M. NORDIC OPTICAL TELESCOPE. GAUSSIAN FOCAL PLANE. ENTR. PUP. RAD.: 1280.0000 F/ 11.000 HALF FIELD: 15.0000 ARC-MIN

Table with 11 columns: THETA, YG, KG, DLMIN, YGMIN, KGMIN, C1, C2, PIO, P11, P12. Rows represent theta values from 0.00 to 15.00.

PROPOSED 2.56-M. NORDIC OPTICAL TELESCOPE. FIELD 5 ARCMIN DIAM. OPTIM. ENTR. PUP. RAD.: 1280.0000 F/ 11.000 HALF FIELD: 15.0000 ARC-MIN

Table with 11 columns: THETA, YG, KG, DLMIN, YGMIN, KGMIN, C1, C2, PIO, P11, P12. Rows represent theta values from 0.00 to 15.00.

PROPOSED 2.56-M. NORDIC OPTICAL TELESCOPE. FIELD 10 ARCMIN DIAM. OPTIM. ENTR. PUP. RAD.: 1280.0000 F/ 11.000 HALF FIELD: 15.0000 ARC-MIN

Table with 11 columns: THETA, YG, KG, DLMIN, YGMIN, KGMIN, C1, C2, PIO, P11, P12. Rows represent theta values from 0.00 to 15.00.

PROPOSED 2.56-M. NORDIC OPTICAL TELESCOPE. FIELD 15 ARCMIN DIAM. OPTIM. ENTR. PUP. RAD.: 1280.0000 F/ 11.000 HALF FIELD: 15.0000 ARC-MIN

Table with 11 columns: THETA, YG, KG, DLMIN, YGMIN, KGMIN, C1, C2, PIO, P11, P12. Rows represent theta values from 0.00 to 15.00.

PROPOSED 2.56-M. NORDIC OPTICAL TELESCOPE. FIELD 20 ARCMIN DIAM. OPTIM. ENTR. PUP. RAD.: 1280.0000 F/ 11.000 HALF FIELD: 15.0000 ARC-MIN

Table with 11 columns: THETA, YG, KG, DLMIN, YGMIN, KGMIN, C1, C2, PIO, P11, P12. Rows represent theta values from 0.00 to 15.00.

PROPOSED 2.56-M. NORDIC OPTICAL TELESCOPE. FIELD 25 ARCMIN DIAM. OPTIM. ENTR. PUP. RAD.: 1280.0000 F/ 11.000 HALF FIELD: 15.0000 ARC-MIN

Table with 11 columns: THETA, YG, KG, DLMIN, YGMIN, KGMIN, C1, C2, PIO, P11, P12. Rows represent theta values from 0.00 to 15.00.

PROPOSED 2.56-M. NORDIC OPTICAL TELESCOPE. FIELD 30 ARCMIN DIAM. OPTIM. ENTR. PUP. RAD.: 1280.0000 F/ 10.999 HALF FIELD: 15.0000 ARC-MIN

Table with 11 columns: THETA, YG, KG, DLMIN, YGMIN, KGMIN, C1, C2, PIO, P11, P12. Rows represent theta values from 0.00 to 15.00.

## 6. TILT-COMPENSATION OF TRANSLATIONAL SHIFT OF THE SECONDARY MIRROR

### 6.1. Introduction and presentation of notation

During the design of the mounting and control system for the secondary mirror for the 2.5 m Nordic Optical Telescope, the question was raised if a translational displacement of the secondary of the order 0.3 mm to 0.5 mm, perpendicular to the optic axis, could eventually be compensated by a controlled tilt of the secondary mirror axis of symmetry, thus to a high degree restoring the imaging properties of the Ritchey-Chrétien telescope. This principle is well-known in optical engineering, c.f., e.g., Meinel and Meinel (1984), and Wetherell and Rimmer (1972).

With this purpose in mind the 2.5 m telescope mirror configuration was investigated by means of a ray tracing computer program, using 3-dimensional ray tracing for generally skew rays. The computer program was designed so as to allow for a displacement of the secondary in a plane perpendicular to the axis of the primary, and to allow for a tilt of the secondary mirror. The displacement is specified by coordinates  $(x_s, y_s)$  of the vector in the plane of displacement from the primary axis to the secondary vertex. The tilt of the secondary is specified by the direction tangents  $(\xi_s, \eta_s)$  of the tilted secondary mirror axis with respect to the primary axis, and the vector

$$(1 + \xi_s^2 + \eta_s^2)^{-\frac{1}{2}} (\xi_s, \eta_s, 1)$$

is a unit vector on the secondary mirror axis referred to the primary coordinate system. Furthermore

$$\cos \phi = (1 + \xi_s^2 + \eta_s^2)^{-\frac{1}{2}} \quad (6-1)$$

where  $\phi$  is the angle between the mirror axes.

For reasons of symmetry it is clear that a tilt aimed at compensating a given displacement must be in the same direction as the displacement, i.e., the vectors  $(x_s, y_s)$  and  $(\xi_s, \eta_s)$  must be linearly dependent. Hence, it is sufficient to describe the displacement by  $y_s$  and the tilt by  $\eta_s$ .

## 6.2. Paraxial analysis

Before proceeding to the ray trace results we perform an analytic first-order description to obtain a rough idea of what to expect when displacing and tilting the secondary mirror. We shall assume that the displacement  $(x_s, y_s)$  and tilt  $(\xi_s, \eta_s)$  are small quantities, and we consider rays in the paraxial limit. The analysis is based on a paper by Andersen (1986) giving equations for the detailed analysis of decentering and tilt of surfaces in a rotationally symmetric system.

With  $(x_1, y_1; \xi_1, \eta_1)$  we denote ray coordinates (intersections and direction tangents) of a ray incident on the primary mirror tangent plane. Similarly, we let  $(x_3, y_3; \xi_3, \eta_3)$  denote the ray coordinates at the image plane. Then, in the paraxial limit, we have

$$\begin{bmatrix} x_3 & y_3 \\ \xi_3 & \eta_3 \end{bmatrix} = \begin{bmatrix} 2d_2 \\ 2 \end{bmatrix} \begin{bmatrix} \xi_s & \eta_s \end{bmatrix} + \begin{bmatrix} \frac{2d_2}{r_2} \\ \frac{2}{r_2} \end{bmatrix} \begin{bmatrix} x_s & y_s \end{bmatrix} \quad (6-2)$$

$$+ \begin{bmatrix} 1 - \frac{2d_2}{r_2} & -d_2 \\ -\frac{2}{r_2} & -1 \end{bmatrix} \begin{bmatrix} 1 - \frac{2d_1}{r_1} & -d_1 \\ -\frac{2}{r_1} & -1 \end{bmatrix} \begin{bmatrix} x_1 & y_1 \\ \xi_1 & \eta_1 \end{bmatrix}$$

where the parameters  $(r_1, r_2; d_1, d_2)$  of the telescope enter in an obvious notation. The last matrix product of Eq. (6-2) is the

paraxial contribution from the ideally centered telescope. Clearly, Eq. (6-2) supports the above conclusion that the vectors  $(x_s, y_s)$  and  $(\xi_s, \eta_s)$  be proportional in order to compensate displacement with tilt. Furthermore, we get a first approximation to the tilt:

$$\begin{bmatrix} \xi_s \\ \eta_s \end{bmatrix} = -\frac{1}{r_2} \begin{bmatrix} x_s \\ y_s \end{bmatrix} \quad (6-3)$$

With the present telescope configuration we have

$$(r_1, r_2; d_1, d_2) = (-10240, -2287.248; -4184.308, 5146.308) \quad (6-4)$$

measured in mm units, and hence

$$-\frac{1}{r_2} = 4.372 \times 10^{-4} \text{ rad/mm} = 90.2 \text{ arcsec/mm} \quad (6-5)$$

Also, from Eq. (6-2) we see that a linear displacement  $(x_s, y_s)$  causes the images all over the field to move an amount

$$\begin{bmatrix} \Delta x_3 \\ \Delta y_3 \end{bmatrix} = \frac{2d_2}{r_2} \begin{bmatrix} x_s \\ y_s \end{bmatrix} = -4.500 \begin{bmatrix} x_s \\ y_s \end{bmatrix} \quad (6-6)$$

and a tilt  $(\xi_s, \eta_s)$  causes the images to move an amount

$$\begin{bmatrix} \Delta x_3 \\ \Delta y_3 \end{bmatrix} = 2d_2 \begin{bmatrix} \xi_s \\ \eta_s \end{bmatrix} = 0.0499 \text{ mm/arcsec} \begin{bmatrix} \xi_s \\ \eta_s \end{bmatrix} \quad (6-7)$$

### 6.3. Ray trace results

The detailed results from the ray tracing computations first slightly modify the figures presented above. Thus, a displacement  $(x_s, y_s)$  causes the images to move an amount

$$\begin{bmatrix} \Delta x_3 \\ \Delta y_3 \end{bmatrix} = -4.416 \begin{bmatrix} x_s \\ y_s \end{bmatrix} \quad (6-8)$$

whereas a tilt  $(\xi_s, \eta_s)$  causes the images to move

$$\begin{bmatrix} \Delta x_3 \\ \Delta y_3 \end{bmatrix} = 0.0495 \text{ mm/arcsec} \begin{bmatrix} \xi_s \\ \eta_s \end{bmatrix} \quad (6-9)$$

Thus, the tilt compensating a certain displacement  $(x_s, y_s)$  is

$$\begin{bmatrix} \xi_s \\ \eta_s \end{bmatrix} = 4.322 \times 10^{-4} \text{ rad/mm} \begin{bmatrix} x_s \\ y_s \end{bmatrix} = 89.1 \text{ arcsec/mm} \begin{bmatrix} x_s \\ y_s \end{bmatrix} \quad (6-10)$$

Furthermore, the ray trace results show that a displacement of 0.5 mm or less does not severely disturb the imaging in the far-field region. The very good on-axis imaging of the RC-telescope is, however, disturbed with an rms image radius of 0.48 arcsec/mm displacement. The major obstacle is, of course, the displacement of the images according to Eq. (6-8).

In the following we present results of ray tracing calculations for various values of the displacement  $y_s$  with a compensating tilt  $\eta_s$  adopted according Eq. (6-10). The field of view was scanned along both the  $\xi_1$ -axis and the  $\eta_1$ -axis from -20' to +20' with 1' step for both object axes. The image plane was fixed

as the paraxial image plane for the ideal telescope, and the distance  $d_1$  between the mirrors was fixed to the ideal value for paraxial imagery. The computer program calculated the center of gravity  $(x_g, y_g)$  of the geometric image and the rms image radius  $k_g$  of the ray distribution according to methods developed by Andersen (1981a, 1982a). Denoting by

$$I_{\omega}(F) = \frac{1}{a_{\omega}} \iint_{\omega} F(x_1, y_1) dx_1 dy_1 \quad (6-11)$$

the average value of a quantity  $F$  over the entrance pupil  $\omega$ , the following quantities were computed numerically:

$$\begin{aligned} S_1 &= I_{\omega}(x_3) \\ S_2 &= I_{\omega}(\xi_3) \\ S_3 &= I_{\omega}(y_3) \\ S_4 &= I_{\omega}(\eta_3) \\ S_5 &= I_{\omega}(x_3\xi_3 + y_3\eta_3) \\ S_6 &= I_{\omega}(\xi_3^2 + \eta_3^2) \\ S_7 &= I_{\omega}(x_3^2 + y_3^2) \end{aligned} \quad (6-12)$$

where  $x_3, y_3, \xi_3, \eta_3$  are evaluated at the paraxial image plane. The center of gravity  $(x_g, y_g)$  and the rms image radius  $k_g$  for the image at this plane are then

$$\begin{aligned} x_g &= S_1 \quad ; \quad y_g = S_3 \\ k_g^2 &= S_7 - S_1^2 - S_3^2 \end{aligned} \quad (6-13)$$

For an arbitrary image plane shifted the amount  $\Delta$  from the image plane under consideration, we have

$$\begin{aligned} x_g(\Delta) &= S_1 + S_2\Delta \quad ; \quad y_g(\Delta) = S_3 + S_4\Delta \\ k_g^2(\Delta) &= S_7 - S_1^2 - S_3^2 + 2(S_5 - S_1S_2 - S_3S_4)\Delta + (S_6 - S_2^2 - S_4^2)\Delta^2 \end{aligned} \quad (6-14)$$

It is seen, that  $k_g^2$  is a quadratic function of  $\Delta$ , and thus a value  $\Delta_{\min}$  exists for which  $k_g^2$  is a minimum. The corresponding values of  $x_g$ ,  $y_g$  and  $k_g$  are denoted  $x_{g \min}$ ,  $y_{g \min}$  and  $k_{g \min}$ . The following Tables 3-11 display the value of  $\xi_1$  or  $\eta_1$ ,  $x_g$ ,  $y_g$ ,  $k_g$ ,  $\Delta_{\min}$ ,  $x_{g \min}$ ,  $y_{g \min}$ ,  $k_{g \min}$ , and the quantities  $S_2$ ,  $S_4$ ,  $S_5$ ,  $S_6$ . Table 3 presents data for the idealized telescope ( $y_s = 0$ ,  $\eta_s = 0$ ). In order to make a just comparison with Table 2, it is noted that the present averages are carried out over the annular pupil (240, 1270) whereas the averages in Table 2 are over the full circular pupil. Tables 4 through 11 present the data for values of  $y_s$  from 0.1 mm to 0.8 mm with tilt values  $\eta_s$  adopted from Eq. (6-10).

#### 6.4. Conclusions

From Tables 3-11 it is seen that it is possible virtually to restore the imaging within a field of radius 5 arcmin without any change in focal length, and within the defocussing range of interest. It is stressed, however, that the excellent imaging of the on-axis image is somewhat smeared out. Also, for larger field sizes, the effects of decentering and tilt are almost insignificant. Thus, we conclude that it is indeed possible to compensate secondary mirror displacement with tilt of the secondary, at least for displacements up to about 0.5 mm.

We emphasize, however, that the tilt depends on the magnitude of the displacement. Therefore, in order to control the tilt continuously by computer, in particular when guiding during a long exposure, the mechanical repeatability of the secondary displacement must be considered in mechanical investigations of the secondary mounting and be found at an acceptable level. Also, temperature effects on the secondary mirror displacement must be at an absolute minimum.

Further effects of this secondary displacement and tilt on the telescope alignment system have to be investigated separately, possibly implying that alignment of the mirrors must be carried out with the telescope pointing at zenith.



Table 4.  $y_s = 0.1 \text{ mm}$  .  $\eta_s = 0.0000432$

Table with columns labeled  $\xi_1, \eta_1$ ,  $x_g$ ,  $y_g$ ,  $k$ ,  $\Delta_{\min}$ ,  $x_{g \min}$ ,  $y_{g \min}$ ,  $k_{g \min}$ ,  $S_2$ ,  $S_4$ ,  $S_5$ ,  $S_6$ . The table contains numerical data for various parameters across multiple rows.

Table 5.  $y_s = 0.2 \text{ mm}$  .  $\eta_s = 0.0000864$

Table with columns labeled  $\xi_1, \eta_1$ ,  $x_g$ ,  $y_g$ ,  $k_g$ ,  $\Delta_{\min}$ ,  $x_{g \min}$ ,  $y_{g \min}$ ,  $k_{g \min}$ ,  $S_2$ ,  $S_4$ ,  $S_5$ ,  $S_6$ . The table contains multiple rows of data, with some rows showing significant noise or artifacts, particularly in the middle and lower sections.



Table 7.  $y_s = 0.4 \text{ mm}$  .  $\eta_s = 0.0001729$

Table with columns labeled  $\xi_1, \eta_1$ ,  $xg$ ,  $yg$ ,  $kg$ ,  $\Delta_{min}$ ,  $x_{g \text{ min}}$ ,  $y_{g \text{ min}}$ ,  $k_{g \text{ min}}$ ,  $S_2$ ,  $S_4$ ,  $S_5$ ,  $S_6$ . The table contains multiple rows of data, including numerical values and vertical lines, representing experimental or calculated results for different parameters.









7. ASSESSMENT OF THE EFFECTS ON THE GEOMETRIC IMAGE QUALITY  
DUE TO DEFORMATIONS OF THE TELESCOPE MIRRORS

7.1. Introduction

In the mechanical design of support systems for large astronomical telescope mirrors it is of importance to evaluate the influence on the imaging properties by deformations of the optical surfaces in different pointing positions of the telescope, so as to assure that the prescribed image error budget can be fulfilled.

We shall consider the deformations as differential (small first-order) corrections to the idealized optical surfaces and develop formulas for calculating corrections to geometrical rays through the system as well as corrections to the optical path length. We use the notation of Section 2.

7.2. Derivation of equations

In Fig. 7.1 we consider a ray incident on the idealized optical surface  $S$  described by the surface equation

$$z - z_0 = f(x, y). \quad (7-1)$$

The ray is specified by the intersection  $P(x, y)$  with the polar plane  $z = z_0$  and a unit direction vector  $\vec{\sigma} = (L, M, N)$ . The intersection point  $\tilde{P}(\tilde{x}, \tilde{y})$  with the surface is determined by

$$\begin{aligned} \tilde{x} &= x + \xi f(\tilde{x}, \tilde{y}) \\ \tilde{y} &= y + \eta f(\tilde{x}, \tilde{y}) \end{aligned} \quad (7-2)$$

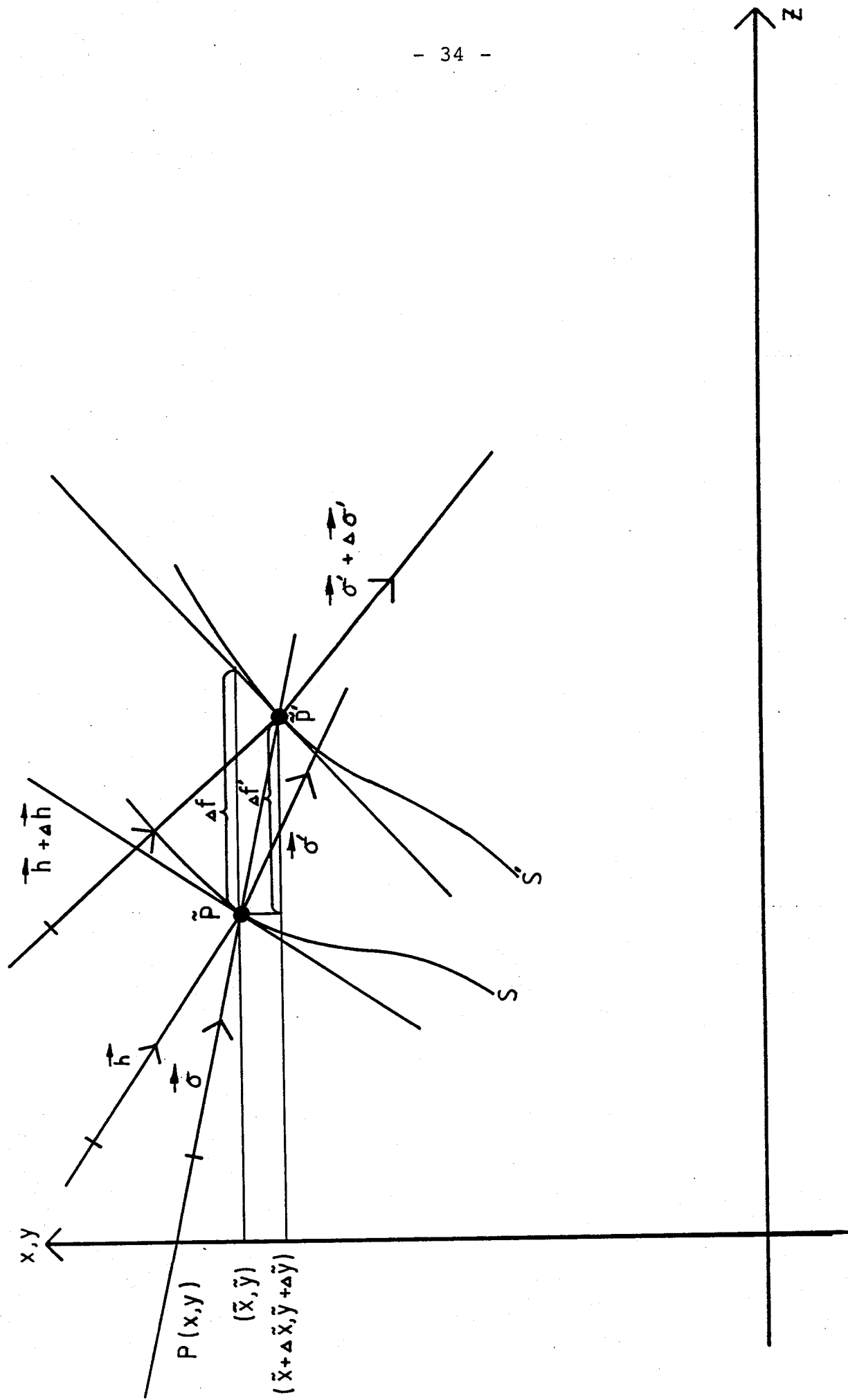


Fig. 7-1. Ray path through an optical surface which is slightly deformed.

$Z = Z_0$

where

$$\xi = \frac{L}{N}, \quad \eta = \frac{M}{N} \quad (7-3)$$

are the direction tangents of the ray.

A unit vector on the surface normal through  $\tilde{P}$  is

$$\vec{h} = (\alpha, \beta, \gamma) = \left(1 + \left(\frac{\partial f}{\partial x}\right)^2 + \left(\frac{\partial f}{\partial y}\right)^2\right)^{-\frac{1}{2}} \left(-\frac{\partial f}{\partial x}, -\frac{\partial f}{\partial y}, 1\right). \quad (7-4)$$

The angle  $\theta$  between  $\vec{\sigma}$  and  $\vec{h}$  is determined by

$$\cos \theta = \vec{\sigma} \cdot \vec{h}, \quad (7-5)$$

and the angle  $\theta'$  between the refracted ray  $\vec{\sigma}'$  and  $\vec{h}$  is determined by

$$\cos \theta' = (1 - \mu^2 + \mu^2 \cos^2 \theta)^{\frac{1}{2}} \quad (7-6)$$

where  $\mu$  is the relative index of refraction. A unit vector on the refracted ray is then

$$\vec{\sigma}' = \mu \vec{\sigma} + (\cos \theta' - \mu \cos \theta) \vec{h} = (L', M', N') \quad (7-7)$$

Finally, the intersection of the refracted ray with the polar plane  $z = z_0 + d$  at the next surface is determined as

$$\begin{bmatrix} x' \\ y' \end{bmatrix} = \begin{bmatrix} \tilde{x} \\ \tilde{y} \end{bmatrix} + (d-f) \begin{bmatrix} \xi' \\ \eta' \end{bmatrix}. \quad (7-8)$$

Consider now the deformed surface  $S'$  given by

$$z - z_0 = f(x, y) + \Delta f(x, y) \quad (7-9)$$

where the deformation  $|\Delta f|$  is considered to be small compared to  $|f|$ , and the gradient  $(\partial \Delta f / \partial x, \partial \Delta f / \partial y)$  is considered to be small compared to the gradient  $(\partial f / \partial x, \partial f / \partial y)$ .

Let the ray intersection point with the deformed surface  $S'$  be  $\tilde{P}'$  ( $\tilde{x} + \Delta\tilde{x}$ ,  $\tilde{y} + \Delta\tilde{y}$ ,  $f(\tilde{x}, \tilde{y}) + \Delta f'$ ). Then we have

$$\tilde{x} + \Delta\tilde{x} = x + \xi(f(\tilde{x}, \tilde{y}) + \Delta f') = \tilde{x} + \xi\Delta f' \quad (7-10)$$

$$\tilde{y} + \Delta\tilde{y} = y + \eta(f(\tilde{x}, \tilde{y}) + \Delta f') = \tilde{y} + \eta\Delta f'$$

The surface normal to  $S'$  in  $\tilde{P}'$  is denoted by  $\vec{h} + \Delta\vec{h}$ . In order to determine  $\Delta\tilde{x}$ ,  $\Delta\tilde{y}$ , and  $\Delta f'$  in terms of  $\Delta f$  and  $\Delta\vec{h}$ , we assume that we can accurately approximate the surfaces  $S$  and  $S'$  by their tangential planes in  $\tilde{P}$  and  $\tilde{P}'$ , respectively. This is equivalent to including only terms to the first order in the quantities  $\Delta f$  and  $\Delta\vec{h}$ . We then get, to this accuracy,

$$\Delta f' = \frac{N\gamma}{\cos\theta} \Delta f \quad (7-11)$$

$$\Delta\tilde{x} = \xi\Delta f' \quad (7-12)$$

$$\Delta\tilde{y} = \eta\Delta f'$$

$$\Delta\cos\theta = \vec{\sigma} \cdot \Delta\vec{h} \quad (7-13)$$

$$\Delta\cos\theta' = \frac{\cos\theta}{\cos^2\theta'} \Delta\cos\theta$$

$$\Delta\vec{\sigma}' = \left( \frac{\cos\theta}{\cos^2\theta'} - \mu \right) (\vec{\sigma} \cdot \Delta\vec{h})\vec{h} + (\cos\theta' - \mu\cos\theta)\Delta\vec{h} \quad (7-14)$$

$$\begin{bmatrix} \Delta\xi' \\ \Delta\eta' \end{bmatrix} = \left( \frac{\cos\theta}{\cos^2\theta'} - \mu \right) (\vec{\sigma} \cdot \Delta\vec{h}) \begin{bmatrix} \frac{\alpha - \gamma\xi'}{N'} \\ \frac{\beta - \gamma\eta'}{N} \end{bmatrix} + \frac{\cos\theta' - \mu\cos\theta}{N'} \begin{bmatrix} \Delta\alpha - \xi'\Delta\gamma \\ \Delta\beta - \eta'\Delta\gamma \end{bmatrix} \quad (7-15)$$

and

$$\begin{bmatrix} \Delta x' \\ \Delta y' \end{bmatrix} = \frac{N\gamma}{\cos\theta} \Delta f \begin{bmatrix} \xi - \xi' \\ \eta - \eta' \end{bmatrix} + (d-f) \begin{bmatrix} \Delta\xi' \\ \Delta\eta' \end{bmatrix} \quad (7-16)$$

Since  $\Delta f$  and  $\Delta \vec{h}$  are small quantities, we may set  $N$ ,  $N'$ ,  $\gamma$ ,  $\cos \theta$ , and  $\cos \theta'$  equal to 1, and  $f$  equal to 0, their paraxial limits. Furthermore,  $\Delta \gamma = 0$  so that

$$\vec{\sigma} \cdot \Delta \vec{h} = N(\xi \Delta \alpha + \eta \Delta \beta + \Delta \gamma) \approx \xi \Delta \alpha + \eta \Delta \beta \quad (7-17)$$

Moreover,

$$\alpha \approx -\frac{\partial f}{\partial x}, \quad \beta \approx -\frac{\partial f}{\partial y} \quad (7-18)$$

If the idealized surface function  $f$  has rotational symmetry,

$$f = f(x^2 + y^2) = f(\rho) = a_1 \rho + a_2 \rho^2, \quad (7-19)$$

and we have

$$\alpha = -2\tilde{x} \frac{df}{d\rho}, \quad \beta = -2\tilde{y} \frac{df}{d\rho} \quad (7-20)$$

which in the paraxial limit reduce to

$$\alpha = -2xa_1, \quad \beta = -2ya_1 \quad (7-21)$$

With these approximations Eqns. (7-15) and (7-16) reduce to

$$\begin{bmatrix} \Delta \xi' \\ \Delta \eta' \end{bmatrix} = -(1-\mu)(\xi \Delta \alpha + \eta \Delta \beta) \begin{bmatrix} 2a_1 x + \xi \\ 2a_1 y + \eta \end{bmatrix} + (1-\mu) \begin{bmatrix} \Delta \alpha \\ \Delta \beta \end{bmatrix}, \quad (7-22)$$

and

$$\begin{bmatrix} \Delta x' \\ \Delta y' \end{bmatrix} = \Delta f \begin{bmatrix} \xi - \xi' \\ \eta - \eta' \end{bmatrix} - d(1-\mu)(\xi \Delta \alpha + \eta \Delta \beta) \begin{bmatrix} 2a_1 x + \xi \\ 2a_1 y + \eta \end{bmatrix} + d(1-\mu) \begin{bmatrix} \Delta \alpha \\ \Delta \beta \end{bmatrix} \quad (7-23)$$

respectively.

Denoting by  $n$  and  $n'$  the refractive indices before and after refraction, the optical path length of a ray from the polar plane  $z = z_0$  through the idealized surface to the next polar plane is

$$K = \frac{nf}{N} + \frac{n'(d-f)}{N'} \quad (7-24)$$

For refraction at the deformed surface and applying the same approximations as above, the optical path length is changed to  $K + \Delta K$  where

$$\Delta K = n'(\mu-1) (\Delta f + d(\xi\Delta\alpha + \eta\Delta\beta)) \quad (7-25)$$

### 7.3. Applications to 2.5 m telescope deformation calculations

We will now apply the formulas of Section 7.2 to estimate upper limits of the effects of deformations of the mirror surfaces. We shall make use of very recent deformation calculations by Andersen and Jessen (1985).

The displacement of a ray  $(x_1, y_1, \xi_1, \eta_1)$  due to deformations  $(\Delta f_1, \Delta\alpha_1, \Delta\beta_1)$  of the primary mirror is imaged by the secondary on the image plane  $z = z_3$ . Using paraxial formulas for the ray paths we obtain for the displacement at the image plane

$$\begin{bmatrix} \Delta x_3 & \Delta y_3 \\ \Delta \xi_3 & \Delta \eta_3 \end{bmatrix} = \begin{bmatrix} 1-4d_2a_{12} & -d_2 \\ -4a_{12} & -1 \end{bmatrix} \begin{bmatrix} \Delta x_2 & \Delta y_2 \\ \Delta \xi_2 & \Delta \eta_2 \end{bmatrix}, \quad (7-26)$$

where

$$\begin{bmatrix} \Delta x_2 \\ \Delta y_2 \end{bmatrix} = 2\Delta f_1 \begin{bmatrix} \xi_1 \\ \eta_1 \end{bmatrix} + 2a_{11}\Delta f_1 \begin{bmatrix} x_1 \\ y_1 \end{bmatrix} + 2d_1 \begin{bmatrix} \Delta\alpha_1 \\ \Delta\beta_1 \end{bmatrix}, \quad (7-27)$$

$$+ 2d_1(\xi_1\Delta\alpha_1 + \eta_1\Delta\beta_1) \begin{bmatrix} 2a_{11}x_1 + \xi_1 \\ 2a_{11}y_1 + \eta_1 \end{bmatrix}$$

and

$$\begin{bmatrix} \Delta\xi_2 \\ \Delta\eta_2 \end{bmatrix} = 2(\xi_1\Delta\alpha_1 + \eta_1\Delta\beta_1) \begin{bmatrix} 2a_{11}x_1 + \xi_1 \\ 2a_{11}y_1 + \eta_1 \end{bmatrix} + 2 \begin{bmatrix} \Delta\alpha_1 \\ \Delta\beta_1 \end{bmatrix} . \quad (7-28)$$

To obtain an upper limit to  $|\Delta x_3|$  we used Fig.s 8 (zenith pointing), 15 (horizon pointing), and 18 (30° zenith distance) of Andersen and Jessen to obtain upper (extreme) limits to  $\Delta f_1$ ,  $\Delta\alpha_1$ , and  $\Delta\beta_1$ . To be conservative, we then set

$$|\Delta f_1| \leq 131 \text{ nm} \quad ; \quad |\Delta\alpha_1|, |\Delta\beta_1| \leq 4.0 \times 10^{-7} \text{ rad} \quad . \quad (7-29)$$

Furthermore

$$|x_1| \leq 1280 \text{ mm} \quad ; \quad |\xi_1| \leq 7.3 \times 10^{-3} \text{ rad} \quad . \quad (7-30)$$

From this we estimate

$$|\Delta x_2| \leq 3.37 \times 10^{-3} \text{ mm} \quad ; \quad |\Delta\xi_2| \leq 8.02 \times 10^{-7} \text{ rad} , \quad (7-31)$$

and then

$$|\Delta x_3| \leq 22.7 \times 10^{-3} \text{ mm} = 0.166 \quad . \quad (7-32)$$

To a very good approximation, the displacements are given by the simple expression

$$\begin{bmatrix} \Delta x_3 \\ \Delta y_3 \end{bmatrix} \approx -2f_{RC} \begin{bmatrix} \Delta\alpha_1 \\ \Delta\beta_1 \end{bmatrix} , \quad (7-33)$$

indicating that deformations of the surface are negligible compared to deformations of the surface normals.

The quoted figure of 0".166 for  $\Delta x_3$  covers the worst-case displacement of any ray over the full aperture and 50'-diameter field. Thus, it is reasonably safe to state that the deformations of the primary mirror will not contribute to the image blur with more than 0".35, and that this figure for specific pointings is considerably smaller. Furthermore, it can be reduced significantly by refocusing.

For deformations of the secondary,  $\Delta f_2$ ,  $\Delta \alpha_2$ ,  $\Delta \beta_2$ , the displacement of a ray  $(x_1, y_1, \xi_1, \eta_1)$  is given by

$$\begin{bmatrix} \Delta x_3 \\ \Delta y_3 \end{bmatrix} = 2\Delta f_2 \begin{bmatrix} \xi_2 \\ \eta_2 \end{bmatrix} + 2a_{12}\Delta f_2 \begin{bmatrix} x_2 \\ y_2 \end{bmatrix} + 2d_2 \begin{bmatrix} \Delta \alpha_2 \\ \Delta \beta_2 \end{bmatrix} + 2d_2(\xi_2\Delta \alpha_2 + \eta_2\Delta \beta_2) \begin{bmatrix} 2a_{12}x_2 + \xi_2 \\ 2a_{12}y_2 + \eta_2 \end{bmatrix} \quad (7-34)$$

where  $(x_2, y_2, \xi_2, \eta_2)$  are given by paraxial expressions in  $(x_1, y_1, \xi_1, \eta_1)$ .

Using Fig.s 27, 34 and 36 of Andersen and Jessen we set

$$|\Delta f_2| \leq 70 \text{ nm} ; \quad |\Delta x_2|, |\Delta \beta_2| \leq 3 \times 10^{-7} \text{ rad} \quad (7-35)$$

This leads, in a worst-case estimate, to

$$|\Delta x_3| \leq 3.74 \times 10^{-3} \text{ mm} = 0".027 \quad (7-36)$$

Thus, the deformations of the secondary mirror will not contribute to the total image blur with more than 0".05.

8. REFERENCES

- Andersen, T.B.: 1980, Appl. Opt. 19, 3800.  
("Automatic computation of optical aberration coefficients").
- Andersen, T.B.: 1981a, Appl. Opt. 20, 2754.  
("Automatic computation of optical focal surfaces").
- Andersen, T.B.: 1981b, Appl. Opt. 20, 3263.  
("Optical aberration coefficients: FORTRAN subroutines for symmetrical systems").
- Andersen, T.B.: 1982a, Appl. Opt. 21, 1241.  
("Evaluating rms spot radii by ray tracing").
- Andersen, T.B.: 1982b, Appl. Opt. 21, 1817.  
("Optical aberration functions: derivatives with respect to axial distances for symmetrical systems").
- Andersen, T.B.: 1982c, Appl. Opt. 21, 4040.  
("Optical aberration functions: chromatic aberrations and derivatives with respect to refractive indices for symmetrical systems").
- Andersen, T.B.: 1982d, Report to the NOT Committee, November 1982.  
("Notes on the optical characteristics and performance of the proposed Nordic Optical Telescope (NOT)").
- Andersen, T.B.: 1984a, Report to the NOT Committee, August 1984.  
("Supplementary notes on the optical characteristics and performance of the 2.5 m Nordic Optical Telescope").

- Andersen, T.B.: 1984b, Report to the NOT Committee, December 1984.  
("Note on tilt-compensation of translational shift of the secondary mirror of the 2.5 m Nordic Optical Telescope").
- Andersen, T.B.: 1985, Appl. Opt. 24, 1122.  
("Optical aberration functions: derivatives with respect to surface parameters for symmetrical systems").
- Andersen, T.B.: 1986, in preparation.  
("On the aberrational effects of tilt and decentering in rotationally symmetric systems").
- Andersen, T.B. and Reiz, A.: 1983, Astron. Astrophys. Suppl. Ser. 53, 181.  
("Positions of Stars in Regions of 14 Southern Galactic Clusters").
- Andersen, T.E. and Jessen, N.C.: 1985, NOT Scient. Ass. Tech. Rep. March 1985.  
("Deformation calculations of the primary and secondary mirrors of the Nordic 2.5 m optical telescope").
- Bowen, I.S.: 1967, Ann. Rev. Astron. Astrophys. 5, 45.  
("Astronomical Optics").
- Chrétien, H.: 1922, Rev. d'Opt. 1, 13 and 49.  
("Le télescope de Newton et le télescope aplanétique").
- Gascoigne, S.C.B.: 1973, Appl. Opt. 12, 1419.  
("Recent advances in astronomical optics").
- Meinel, A.B. and Meinel, M.P.: 1984, Opt. Eng. 23, 801.  
("Zero-coma condition for decentered and tilted secondary mirror in Cassegrain/Nasmyth configuration").

Schwarzschild, K.: 1905, Astron. Mitt. Königl. Sternw. Göttingen, No.s 9, 10, 11.

("Untersuchungen zur Geometrischen Optik").

Wetherell, W.B. and Rimmer, M.P.: 1972, Appl. Opt. 11, 2817.

("General analysis of aplanatic Cassegrain, Gregorian, and Schwarzschild telescopes").

Wyman, C.L. and Korsch, D.: 1974a, Appl. Opt. 13, 2064.

("Aplanatic two-mirror telescopes: a systematic study. 1: Cassegrainian configuration").

Wyman, C.L. and Korsch, D.: 1974b, Appl. Opt. 13, 2402.

("Systematic study of aplanatic two-mirror telescopes. 2: The Gregorian configuration").

Wyman, C.L. and Korsch, D.: 1975, Appl. Opt. 14, 992.

("Aplanatic two-mirror telescopes: a systematic study. 3: The Schwarzschild-Couder configuration").

Wynne, C.G.: 1965, Appl. Opt. 4, 1185.

("Field correctors for large telescopes").

Wynne, C.G.: 1968, Astrophys. J. 152, 675.

("Ritchey-Chrétien telescopes and extended-field systems").

Wynne, C.G.: 1972, Progr. in Optics 10, 139.

("Field correctors for astronomical telescopes").

APPENDIX A. ABERRATION COEFFICIENTS

In this Appendix we present, in tabular form, the power series expansion coefficients of the four aberration functions S, T, V, W. A coefficient, e.g.,  $S_{nijk}$ , is the coefficient to the expansion term  $\rho_o^i \psi_o^j \kappa_o^k$ ,  $i+j+k = n$ . We also give the derivatives  $\partial/\partial c_1$ ,  $\partial/\partial c_2$ ,  $\partial/\partial b_1$ ,  $\partial/\partial b_2$  with respect to paraxial curvatures and aspheric parameters. We present terms only to the 5th order, since terms of 7th and higher orders are negligible for this optical system.

n i j k	S	$\delta S/\delta c1$	$\delta S/\delta c2$	$\delta S/\delta b1$	$\delta S/\delta b2$
0 0 0 0	-8.53355E-09	5.63200E+04	-1.88100E+03	0.00000E+00	0.00000E+00
1 1 0 0	1.69139E-16	-1.08613E-03	4.38749E-05	-2.62260E-08	2.62510E-09
1 0 1 0	-1.20944E+01	3.01472E+05	4.10840E+04	0.00000E+00	1.37615E+00
1 0 0 1	8.56843E-12	-5.85084E+01	2.40179E+00	0.00000E+00	1.20209E-04
2 2 0 0	4.98569E-20	1.59375E-11	-6.40066E-13	3.80713E-16	-3.75412E-17
2 1 1 0	3.02442E-08	2.00618E-02	-1.02767E-03	-1.40384E-07	-7.80419E-08
2 1 0 1	6.83845E-14	1.44975E-06	-5.85745E-08	2.98062E-11	-3.46487E-12
2 0 2 0	-6.02518E+01	1.59815E+06	3.39013E+05	0.00000E+00	-2.39860E+01
2 0 1 1	1.29029E-02	-9.49061E+02	-5.11973E+01	0.00000E+00	-4.46126E-03
2 0 0 2	1.57933E-08	5.38518E-02	-2.28602E-03	0.00000E+00	-1.30704E-07

n i j k	T	$\delta T/\delta c1$	$\delta T/\delta c2$	$\delta T/\delta b1$	$\delta T/\delta b2$
0 0 0 0	2.81600E+04	0.00000E+00	-4.30675E+07	0.00000E+00	0.00000E+00
1 1 0 0	1.39164E-12	-1.01307E+01	5.62199E-01	0.00000E+00	6.01043E-05
1 0 1 0	1.50736E+05	0.00000E+00	-6.84160E+08	0.00000E+00	3.15084E+04
1 0 0 1	-5.06535E+00	6.59264E+05	-3.39925E+03	0.00000E+00	2.75230E+00
2 2 0 0	1.70961E-14	2.53377E-07	-1.03944E-08	5.35776E-12	-6.56639E-13
2 1 1 0	1.69259E-04	-4.35828E+02	1.86592E+01	0.00000E+00	3.69826E-04
2 1 0 1	1.57933E-08	-7.55627E-03	1.98171E-04	-3.06994E-07	-7.52973E-09
2 0 2 0	7.99073E+05	0.00000E+00	-5.47448E+09	0.00000E+00	5.25646E+05
2 0 1 1	-2.09334E+02	7.29700E+06	1.25868E+06	0.00000E+00	2.45125E+01
2 0 0 2	1.12015E-03	-8.57599E+02	2.61802E+01	0.00000E+00	-1.30103E-04

n i j k	V	$\delta V/\delta c1$	$\delta V/\delta c2$	$\delta V/\delta b1$	$\delta V/\delta b2$
0 0 0 0	-3.55114E-05	9.31763E+00	-3.65505E-01	0.00000E+00	0.00000E+00
1 1 0 0	-2.23909E-14	-2.05344E-07	8.29506E-09	-4.33886E-12	5.10093E-13
1 0 1 0	-2.17845E-03	5.01631E+01	7.86238E-00	0.00000E+00	2.67406E-04
1 0 0 1	-5.12662E-10	-1.11000E-02	4.56148E-04	0.00000E+00	2.33582E-08
2 2 0 0	8.63037E-24	3.18865E-15	-1.28065E-16	7.57389E-20	-7.49581E-21
2 1 1 0	1.01701E-11	4.02235E-06	-2.18750E-07	-2.33590E-11	-1.53754E-11
2 1 0 1	1.10268E-17	2.93530E-10	-1.18631E-11	5.59254E-15	-6.91683E-16
2 0 2 0	-9.95083E-03	2.66528E+02	5.63182E+01	0.00000E+00	-4.71607E-03
2 0 1 1	2.51671E-06	-1.65071E-01	-1.08195E-02	0.00000E+00	-8.76537E-07
2 0 0 2	2.99945E-12	4.07123E-05	-4.54048E-07	0.00000E+00	-2.58190E-11

n i j k	W	$\delta W/\delta c1$	$\delta W/\delta c2$	$\delta W/\delta b1$	$\delta W/\delta b2$
0 0 0 0	4.65881E+00	0.00000E+00	-8.36862E+03	0.00000E+00	0.00000E+00
1 1 0 0	-1.23142E-08	-2.42169E-03	1.39478E-04	0.00000E+00	1.16791E-08
1 0 1 0	2.50816E+01	0.00000E+00	-1.17092E+05	0.00000E+00	6.12253E+00
1 0 0 1	-1.19309E-03	1.09644E+02	7.23989E-01	0.00000E+00	5.34811E-04
2 2 0 0	1.50599E-17	5.98898E-11	-2.45931E-12	1.22535E-15	-1.56976E-16
2 1 1 0	6.31180E-10	-8.01222E-02	3.51739E-03	0.00000E+00	4.10566E-08
2 1 0 1	4.67536E-12	-8.68774E-07	1.33935E-08	-5.10569E-11	-4.15407E-12
2 0 2 0	1.33264E+02	0.00000E+00	-9.23660E+05	0.00000E+00	9.40657E+01
2 0 1 1	-3.83753E-02	1.21660E+03	2.37493E+02	0.00000E+00	3.35245E-03
2 0 0 2	3.23238E-07	-1.58274E-01	4.27417E-03	0.00000E+00	-8.68926E-08

